Comparison of radar rainfall estimates and raingage measurements over the Central Apennines (*)

E. GORGUCCI ([1]), G. SCARCHILLI ([1]) and V. CHANDRASEKAR ([2])
([1]) *Istituto di Fisica dell'Atmosfera (CNR) - Roma, Italy*
([2]) *Colorado State University - Fort Collins, Colorado, USA*

(ricevuto il 21 Ottobre 1996; revisionato il 5 Agosto 1997; approvato il 25 Settembre 1997)

Summary. — Radar measurement of rainfall over mountainous regions is a difficult task due to the requirements of avoiding beam blockage as well as contamination by the melting layer. In this paper the raingage measurements and radar estimates of rainfall over two distinct locations in the central Apennines are compared to study the effect of beam blocking on radar measurements. A simple procedure is developed to estimate the percentage of beam blockage by the mountain ridges and, correspondingly, to correct the radar estimates of rainfall.

PACS 92.60.Jq – Water in the atmosphere (humidity, clouds, evaporation, precipitation).

1. – Introduction

Radar measurement of rainfall over mountainous regions is a challenging task. Radar scans have to be done at fairly low elevation angles to avoid contamination of radar echoes from the melting layer. At the same time, low-elevation radar scans suffer from ground clutter contamination and blockage of radar beam from elevated ground targest or mountains. Contamination from ground clutter can be removed fairly easily using ground clutter filters. However, no processing procedure can recover the blocked echo. When the beam is completely blocked by mountains there will be no radar echo received from the farther targets in range and this feature can be easily spotted on radar pictures. However, when the beam is partially blocked the echo received from the ranges farther than the blocking target will be reduced and the radar reflectivity (Z_H) will be correspondingly reduced in proportion to the amount of beam blockage. Partially blocked beams may not be easily observed on a radar map because it is difficult to distinguish between a partially blocked echo from a strong target and a weaker weather echo. The river basins in the Apennines in Central Italy have several mountain ridges and radar observations over the river basins potentially suffer from the beam blockage problems. Nevertheless, radar estimates of rainfall need to be obtained over the river basins for flood forecast applications.

(*) The authors of this paper have agreed to not receive the proofs for correction.

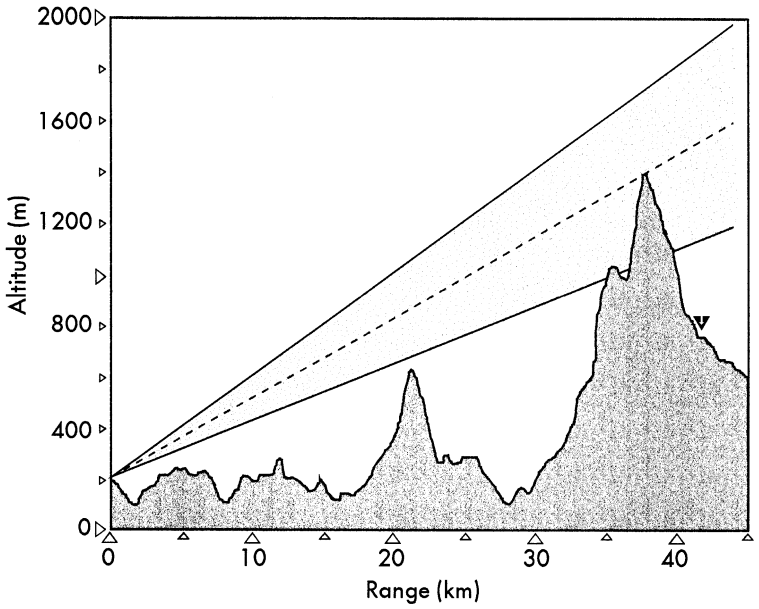

Fig. 1. – Typical altitude profile of the mountains a seen by the radar beam observing precipitation echoes at a fixed azimuth at an elevation of 1.8 degrees.

The radar operational elevation angle for precipitation estimation is selected so that on the average the beam blocking is minimized and at the same time the radar beam does not suffer from contamination of echoes from the melting layer. In the central region of Italy during fall and spring the melting layer of rainstorms is typically above 3 km. This condition suggests that to avoid ice contamination in all ranges up to 100 km the elevation angle should be below 1.7°. However, there are several mountain ridges in the Apennines that have average altitudes of 1500 m at a distance of 50 km from the radar. Figure 1 shows a typical altitude profile of the mountains as seen by a radar beam observing precipitation echoes at a fixed azimuth angle. The operation of the radar is done by compromising between the above two requirements, such that the scans are made at 1.8° elevation.

Comparison of radar and gage measurements are conducted for various purposes such as: i) determination of Z-R relations and ii) validation of radar algorithms. However, extreme care has to be exercised in the interpretation of the comparison between radar and raingage measurements obtained over mountainous terrain. Complete blockage of beams will produce no echoes and it will be easy to detect such situations in the intercomparison. However, rainfall comparisons using data from partially blocked beams can produce errors that are of the same order in the rainfall algorithms using Z-R relations. This paper presents results from the intercomparison of radar and gage measurements from two different regions over the Central Apennines to study the effect of beam blockage in the rainfall estimation algorithms.

Our paper is organized as follows: Section **2** describes rainfall estimation using radar at C-band fequencies; the data presented in our paper is collected using a C-band radar. Radar echoes at C-band are affected by attenuation and a procedure to correct

for attenuation based on dual-polarization measurements is discussed in sect. **3**. Section **4** describes the data set used in our analysis. The comparison between radar and gage estimates of rainfall in the context of beam blockage is presented in sect. **5**. Section **6** summarizes the important results in the paper.

2. – Rainfall estimates at *C*-band

The distribution of raindrop size and shape forms the building block for obtaining the properties of the rain medium such as the reflectivity Z, rainfall rate R and the differential reflectivity Z_{DR}. The gamma distribution model can adequately describe the natural variations in the raindrop size distribution (RSD). This model is given by

$$N(D) = N_0 D^{\mu} \exp\left[\frac{-(3.67+\mu)\,D}{D_0}\right], \tag{1}$$

where N_0, D_0 and μ are the parameters of the RSD and D_0 is the median volume diameter. Rainfall rate R and the radar parameters such as the reflectivity factor at horizontal and vertical polarization $Z_{\mathrm{H,V}}$ and the differential reflectivity Z_{DR} can be expressed in terms of the RSD as follows:

$$R = 0.6\pi \times 10^{-3} \int D^3 N(D)\, v(D)\, \mathrm{d}D\,, \tag{2}$$

where $v(D)$ is the terminal fall speed in still air;

$$Z_{\mathrm{H,V}} = \frac{\lambda^4}{\pi^5 |K|^2} \int \sigma_{\mathrm{H,V}}(D)\, N(D)\, \mathrm{d}D\,, \tag{3}$$

where $\sigma_{\mathrm{H,V}}$ are the radar cross-sections of raindrops at H and V polarization states, λ the wavelength and $K = (\varepsilon_r - 1)/(\varepsilon_r + 2)$, where ε_r is the dielectric constant of water,

$$Z_{\mathrm{DR}} = 10\, \log\left(\frac{Z_{\mathrm{H}}}{Z_{\mathrm{V}}}\right) \tag{4}$$

as suggested by Seliga and Bringi [1].

Utilizing the radar observables Z_{H} and Z_{DR}, two estimates of rainfall rate R can be obtained as follows:

$$R_{\mathrm{ZH}} = C_{\mathrm{ZH}} Z_{\mathrm{H}}^{\nu}\,, \tag{5}$$

$$R_{\mathrm{DR}} = C_{\mathrm{DR}} Z_{\mathrm{H}}^{\alpha} 10^{\beta Z_{\mathrm{DR}}}\,, \tag{6}$$

where C_{ZH}, C_{DR}, ν, α and β are coefficients which depend on the operating wavelength. In the literature (5) is commonly written in an alternate form as

$$Z = aR^{b}\,, \tag{7}$$

where a and b are coefficients for the inverse representation of (5). Scarchilli *et al.* [2] have studied the accuracy of polarization diversity measurements of rainfall at *C*-band

frequencies. Gorgucci *et al.* [3] presented the dual-polarization rainfall algorithm at *C*-band as

$$R_{\mathrm{DR}} = 7.60 \times 10^{-3} Z_{\mathrm{H}}^{0.93} 10^{-0.281 Z_{\mathrm{DR}}} . \tag{8}$$

However, the same simulation can be used to get a representative *Z*-*R* relation, and is given by

$$R_{\mathrm{ZH}} = 2.71 \times 10^{-2} Z_{\mathrm{H}}^{0.71} . \tag{9}$$

It is to be noted here that (9) represents an arbitrary *Z*-*R* relation obtained to provide the best fit for the RSD variabilities studied by Ulbrich [4]. The algorithms given by (8) and (9) are used throughout the various procedures in this paper.

Reflectivity measurements at *C*-band wavelengths are affected by the attenuation of radar signals passing through precipitation that exists between the radar and the measurement cell. Differential reflectivity measurements at *C*-band are similarly affected by the differential attenuation between H and V polarized waves due to propagation through the same precipitation path. The absolute specific attenuation α_{H} (attenuation per unit length) and the specific differential attenuation α_{D} (differential attenuation per unit length) between the two polarizations are related to RSD as follows [5]:

$$\alpha_{\mathrm{H,V}} = 4.343 \times 10^{-3} \ \mathrm{Im} \int_0^\infty f_{\mathrm{H,V}} N(D) \, \mathrm{d}D \, (\mathrm{dB\,km^{-1}}) , \tag{10}$$

$$\alpha_{\mathrm{D}} = \alpha_{\mathrm{H}} - \alpha_{\mathrm{V}} \, (\mathrm{dB\,km^{-1}}) , \tag{11}$$

where $f_{\mathrm{H,V}}$ are the forward-scattering amplitudes at the H and V polarization states, respectively, and Im refers to the imaginary part of a complex number.

Scarchilli *et al.* [2] have studied the variability of $\alpha_{\mathrm{H,V}}$ and α_{D} as a function of rainfall rate at *C*-band frequencies. Their results show that specific attenuation rates can be as high as $0.5\,\mathrm{dB\,km^{-1}}$ and α_{D} can be as much as $0.15\,\mathrm{dB\,km^{-1}}$. These results show that the absolute attenuation through large rain cells could be easily several decibels in magnitude while comparable values of differential attenuation could also reach as much as a few decibels. In the following section we describe an algorithm to correct the *C*-band radar data for attenuation and differential attenuation based on using reflectivity and differential reflectivity.

3. – Attenuation correction procedure using Z_{H} and Z_{DR}

Aydin *et al.* [6] have described a procedure to estimate the attenuation based on Z_{H} and Z_{DR} parameterizing the relation between the ratio $(\alpha_{\mathrm{H}}/Z_{\mathrm{H}})$ and Z_{DR}. A fairly direct (and simpler) approach is presented here to estimate α_{H} and α_{D} based on Z_{H} and Z_{DR}. Similar to the parameterization of rainfall rate given by (6), α_{H} and α_{D} can be parameterized in terms of Z_{H} and Z_{DR}, as

$$\widehat{\alpha}_{\mathrm{H}} = C_{\mathrm{H}} Z_{\mathrm{H}}^{a_1} \times 10^{b_1 Z_{\mathrm{DR}}} , \tag{12}$$

$$\widehat{\alpha}_{\mathrm{D}} = C_{\mathrm{D}} Z_{\mathrm{H}}^{a_2} \times 10^{b_2 Z_{\mathrm{DR}}} . \tag{13}$$

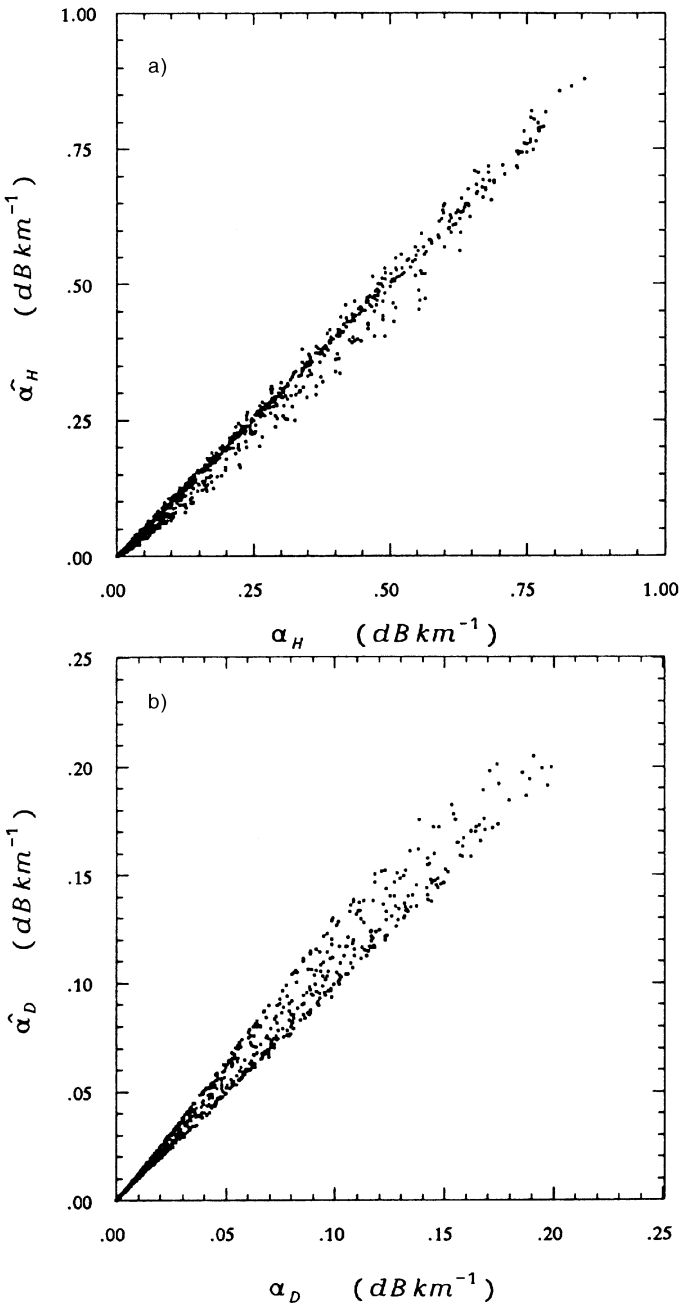

Fig. 2. – a) Scatter plot of the estimate of absolute specific attenuation using Z_H and Z_{DR} as a function of true absolute specific attenuation for different RSD. b) Scatter plot of the estimate differentail attenuation using Z_H and Z_{DR} as a function of true specific differential attenuation for different RSD.

The coefficients C_H, C_D, a_1, a_2, b_1 and b_2 vary with temperature, but not extensively. The coefficients in (12) and (13) at 10 °C are

$$C_H = 6.31 \times 10^{-6}, \quad a_1 = 0.97, \quad b_1 = -0.104,$$

$$C_D = 5.86 \times 10^{-7}, \quad a_2 = 1.02, \quad b_1 = -0.03.$$

The parameterization at 10 °C is used in this paper. Figure 2a) shows a scatter plot of $\widehat{\alpha}_H$ *vs.* α_H, whereas fig. 2b) shows $\widehat{\alpha}_D$ *vs.* α_D. Figures 2a) and 2b) show the ability of the parameterization in (12) and (13) to track the true specific attenuation and differential attenuation. It can be seen that the estimates $\widehat{\alpha}_H$ and $\widehat{\alpha}_D$ follow the actual attenuation values well, with a very narrow scatter and the correlation coefficients are 0.998 and 0.991, respectively.

Attenuation and differential attenuation cumulatively increase with the range. Therefore, echoes from cells close to the radar are not attenuated as much as the echoes from storm cells farther from the radar. It can be assumed that the closest echo is not attenuated and the attenuation cumulatively adds from that point. Therefore, the attenuation is estimated from the first-range echo point and then the reflectivities are corrected sequentially in range. In other words, a cumulative procedure in range is used similar to the one used by Aydin *et al.* [6] to correct for attenuation and differential attenuation. The algorithm for attenuation and differential attenuation correction is as follows:

$$(\widehat{Z}_H)_n = (Z_H^{\text{meas}})_n + \sum_{i=1}^{n-1} (\widehat{\alpha}_H)_i \, \Delta r, \tag{14}$$

where $(\widehat{Z}_H)_n$ is the reflectivity at range bin n corrected for attenuation, $(Z_H^{\text{meas}})_n$ is the measured reflectivity at range bin n, Δr is the range resolution, $(\widehat{\alpha}_H)_i$ is the estimate of the specific attenuation at range bin i. It should be noted here that reflectivity estimate at range $(\widehat{Z}_H)_i$ is corrected for attenuation up to $(i-1)$ range bins. Similarly, the differential reflectivity measurements can be corrected as

$$(\widehat{Z}_{DR})_n = (Z_{DR}^{\text{meas}})_n + \sum_{i=1}^{n-1} (\widehat{\alpha}_D)_i \, \Delta r, \tag{15}$$

where $(\widehat{Z}_{DR})_n$ is the estimate of differential reflectivity at range bin n corrected for differential attenuation, $(Z_{DR}^{\text{meas}})_n$ is the measured differential reflectivity at range bin n and $(\widehat{\alpha}_D)_i$ is the estimate of the specific differential attenuation at range i.

There are potentially two sources of errors that can affect this correction algorithm, namely: *a*) random measurement fluctuations and *b*) error in absolute gain of the radar system (that results as a bias in the estimate of Z_H) as well as a bias in the estimate of Z_{DR}. The effect of random measurement fluctuations were analyzed using simulations and the results show that the random measurement errors do not significantly increase the error in the estimates of $\widehat{\alpha}_H$ and $\widehat{\alpha}_D$. However, bias errors in Z_H can drastically deteriorate the estimates corrected for attenuation, because these errors add cumulatively [6]. The attenuation correction procedure described in this section is applied to the data collected by the Polar 55C, in a storm event over the Central Apennines.

4. – Data description

The radar data, used in this research work, were collected by the dual-polarized *C*-band radar Polar 55C. The Polar 55C is a *C*-band dual-polarization radar, owned by the Institute of Atmospheric Physics (IFA) of the National Research Council (CNR) of Italy and operated jointly with the University of Florence. The radar is located at Montagnana near Florence, Italy. Figure 3 shows a picture of Polar 55C at the operational location. This location provides good radar coverage over the Arno river basin. The Polar 55C is a *C*-band dual-polarized Doppler weather radar with a 0.9° beamwidth. The radar signals are fed to a radar signal processor (SP20, manufactured by Lassen Research, USA) which is capable of providing real-time estimates of reflectivity at horizontal polarization (Z_H) and the differential reflectivity (Z_{DR}). More details about the radar can be found in Scarchilli *et al.* [7]. The Arno basin is also instrumented with a network of tipping bucket raingages. The raingage network is operated by the "Servizio Idrografico e Mareografico" of Pisa, Italy. The rainfall

Fig. 3. – Picture of the radar Polar 55C.

accumulation in the raingages was recorded every 15 minutes with a resolution of 0.2 mm. The experimental region is mountainous and therefore the gages were at various altitudes ranging between sea level and 1400 m. The radar is located at an altitude of 250 m. The data presented in this paper were collected during a precipitation event that occurred on October 30 and 31, 1992 over Central Italy. The associated storm produced intense rainfall over the Central Apennines, creating flood levels in some of the rivers. During this event the Polar 55C was put in an "operational mode" to monitor the basin for hydrological application. This mode consisted of a scan strategy as follows. PPI scans were done over full 360° azimuth angle at a fixed elevation angle of 1.8° at routine time intervals. The melting layer of the storm was determined from soundings at 3.5 km, and therefore most of the radar measurements were in the rain phase of the storms. The time interval between scans was set to be 10 minutes to sample the storm system adequately. The radar measurements were obtained by integrating 64 sample pairs of the echoes with a pulse repetition time (PRT) of 0.85 ms.

Several preprocessing and data reduction procedures were applied to the radar data as described in the following. The radar data were thresholded at −10 dBZ to

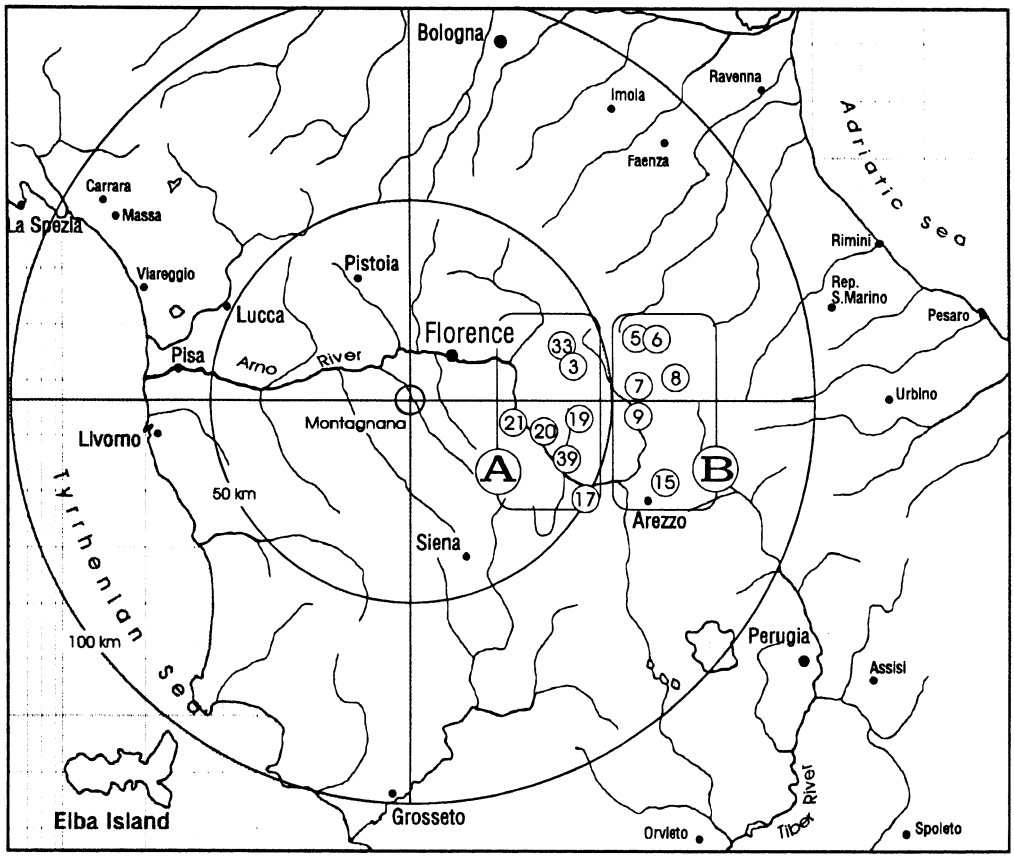

Fig. 4. – Map showing the location of radar, the coverage area over the Arno river basin, the two basins A and B with respect to the radar (0, 0) as well as the position and the ID number of the raingages.

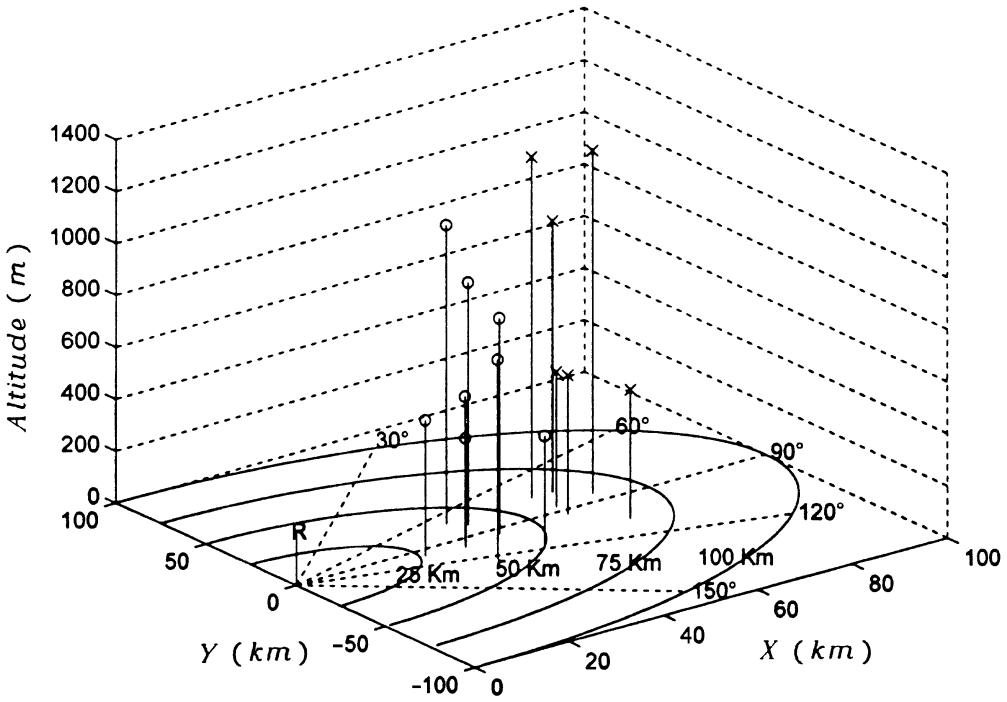

Fig. 5. – Diagram showing the location and the altitude of the raingages with respect to the radar. The circles (○) indicate gages in basin A whereas the (×) symbol indicates gages in basin B.

avoid possible noise contamination. This procedure can potentially remove good data close to the radar, where the −10 dBZ levels could be above noise. However, storm cells at these reflectivity levels do not contribute significantly to rainfall, and therefore can be ignored for our application. Secondly, potential contamination from ice/hail regions was eliminated by thresholding on Z_{DR} values of zero dB, and enforcing an upper limit of 55 dBZ for the reflectivity factor [8]. Again, here the loss of good data points near this boundary is outweighed by potential erroneous data that can bias the rainfall estimates significantly. Thirdly, potentail ground clutter contamination was removed by eliminating data points with zero velocity and near spectrum width, close to the radar. Subsequently, the radar measurements were averaged over nearest neighbors of 1 km each side to reduce measurements error fluctuations.

Radar PPI are obtained nearly instantaneously in comparison with raingage data. With a scan rate of 6 deg/s it takes 1 minute to obtain a PPI, whereas the raingage data are integrated over 15 minutes. Therefore, to enable proper comparison between the radar raingage data the following procedure is adopted: *a*) time series of radar data were constructed at the gage locations from the instantaneous snapshots of the PPIs, *b*) this time series is interpolated and integrated over time to provide synchronization between the radar and raingage data.

Two small basins, approximately 125 km^2 each, were selected for comparative study with radar estimates. One of the basins (basin A) is close to the radar and there are no mountains between the radar and the basin. The second basin (basin B) is farther from the radar with a long mountain ridge of approximately 1500 m in altitude between the

radar and the basin. Figure 4 shows the location of radar, the coverage area of the radar and the two rectangular areas, which are designated as basin A and B. The center of basin A is 35 km from the radar whereas the center of basin B is 65 km from the radar. The effect of beam blockage is expected to be significant over basin B in comparison with basin A because of the long mountain ridge that exists between the radar and the measurement cell over basin B. The various raingage locations and altitudes over basin A and B are shown in fig. 5. In the following section we study the comparison of radar and raingage rainfall measurements in the two basins.

5. – Experimental results

5˙1. *Data analysis procedure.* – The procedure to compute rainfall at a specific gage location using radar data is conceptually straightforward but numerous details are important. The steps involved in processing radar data for comparison with raingage observations are as follows:

a) The location of each raingage is mapped on the radar PPI of reflectivity factor and differentail reflectivity. Subsequently, the radar data are converted to rainfall rate using each of the following two algorithms: i) the Z-R relation given by (9) and ii) the dual polarization algorithm given by (8).

b) The radar estimates are then averaged over its nearest neighbors of one km each side, to obtain average measurements. This is done to filter out the measurement errors. The rainfall obtained from the radar is then averaged over time for each basin and the results are discussed in the following.

A set of three error measurements, namely *a*) the Fractional Standard Error (FSE), *b*) bias and *c*) correlation coefficient are computed to compare the various rainfall algorithms used in this paper. The estimate of the error measure, namely the Fractional Standard Error, can be obtained as

$$\text{FSE} = \frac{\left\{ \dfrac{1}{N_\text{m} N_\text{g}} \displaystyle\sum_{i=1}^{N_\text{g}} \left[\sum_{j=1}^{N_\text{m}} (R_{i,j}^\text{r} - R_{i,j}^\text{g})^2 \right] \right\}}{\dfrac{1}{N_\text{m} N_\text{g}} \displaystyle\sum_{i=1}^{N_\text{g}} \left(\sum_{j=1}^{N_\text{m}} R_{i,j}^\text{g} \right)} , \tag{16}$$

where N_m is the number of measurements for each gage and for a fixed accumulation time, N_g is the number of raingages over the basin, $R_{i,j}^\text{r}$ is the radar rainfall estimate and $R_{i,j}^\text{g}$ the corresponding gage measurement.

The bias in the radar estimates of rainfall (in comparison to the gage estimates) is studied in terms of the relative mean rainfall difference as

$$\text{bias} = \frac{\displaystyle\sum_{i=1}^{N_\text{g}} \left(\sum_{j=1}^{N_\text{m}} R_{i,j}^\text{g} \right) - \sum_{i=1}^{N_\text{g}} \left(\sum_{j=1}^{N_\text{m}} R_{i,j}^\text{r} \right)}{\displaystyle\sum_{i=1}^{N_\text{g}} \left(\sum_{j=1}^{N_\text{m}} R_{i,j}^\text{g} \right)} . \tag{17}$$

The FSE parameter that measures the absolute difference between the radar and gage estimates (inclusive of bias and random scatter) is studied in detail as a function of

the temporal averaging in the rainfall estimation process. The other measures, namely bias and correlation coefficient, are presented only for 30 min rainfall accumulation estimates for the sake of brevity. Thus the FSE, bias, and the correlation between the radar and raingage estimates of rainfall are used to compare the radar rainfall estimates with gage measurements.

5·2. *Comparative analysis of radar rainfall estimates for basins* A *and* B. – The intercomparison of radar and gage measurements of the rainfall is studied in this section for the algorithms R_{DR} and R_{ZH} as a function of temporal averaging units.

The FSE evaluation of temporal averaging is done as follows:

i) the data from several gages in each basin, as well as the corresponding radar data over time are arranged in a matrix, such that each row corresponds to observations from one gage and each column corresponds to observations from different gages at the same time;

ii) the data are then averaged over the consecutive time intervals to obtain the temporally averaged estimates, where the extent of averaging (or the number of units averaged) is the same. Subsequently, the averaged estimates are used in the analysis.

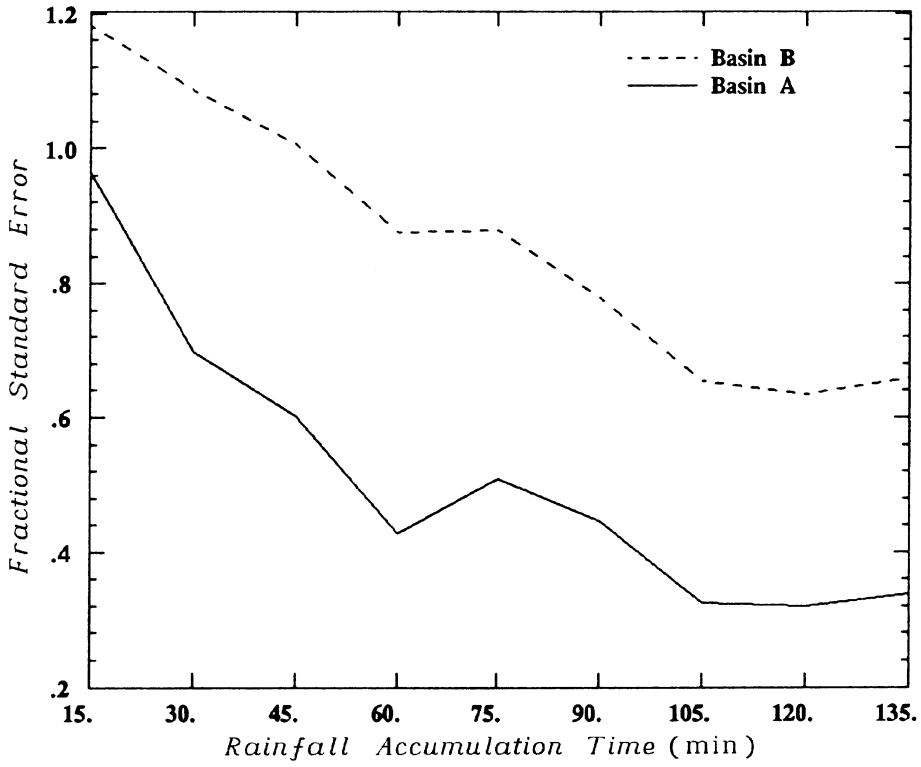

Fig. 6. – Fractional standard error of rainfall over the basins A and B for the R_{ZH} algorithm shown as a function of the rainfall accumulation time.

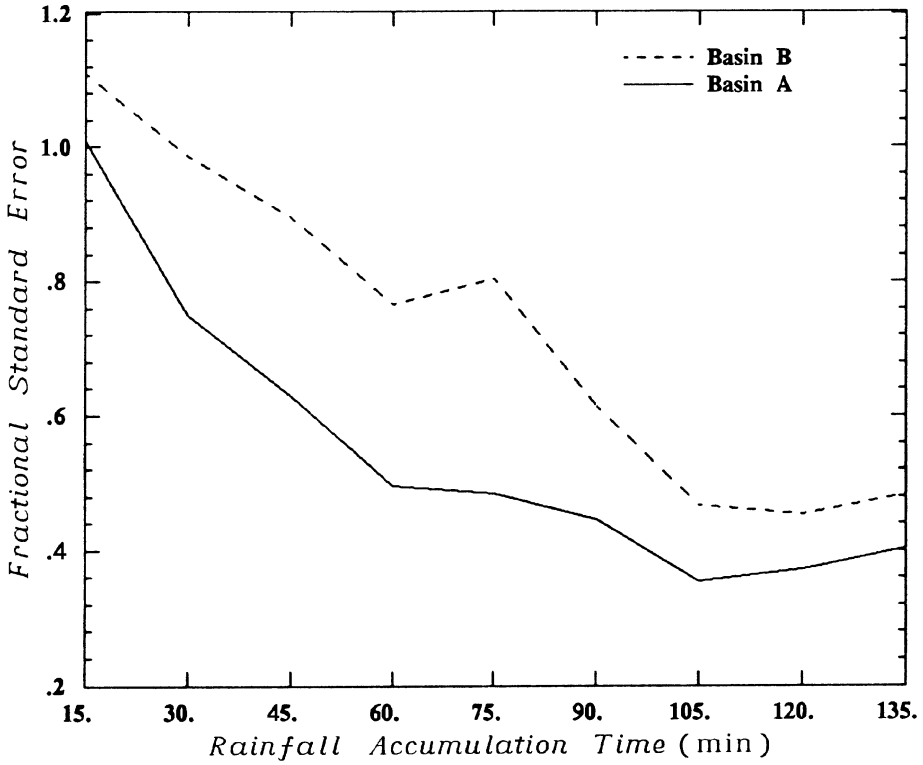

Fig. 7. – Fractional standard error of rainfall over the basins A and B for the R_{DR} algorithm shown as a function of the rainfall accumulation time.

Figures 6, 7 show th FSE of rainfall for the various algorithms as a function of the rainfall accumulation time for the two basins. For proper comparison the radar data were also averaged in the same way the raingage data were averaged. Figure 6 shows the FSE results of R_{ZH} over basins A and B. Similarly, fig. 7 shows the results for basin A and B using R_{DR} algorithm.

Several observations can be made from figs. 6 and 7. On the average, the radar estimates perform worse over basin B in comparison to basin A. The differences in the performance of the radar rainfall algorithms over basin A and B can be easily understood with an examination of the intercepting mountain altitude profile at the azimuth angles of the various gage locations for the two basins.

Table I shows the bias of the mean rainfall estimates, the correlation coefficient and FSE for two rainfall algorithms for both basins at 30 min rainfall accumulations. We can see that for basin A, R_{ZH} and R_{DR} estimates have nearly the same mean rainfall as the gage measurements, whereas for basin B the two rainfall algorithms have significant bias in the estimate of the mean. A similar observation can be made about the correlation coefficient between radar and gage estimates. The correlation coefficient for basin A is uniformly higher than that of basin B for both algorithms. The results of FSE shown in table I represent a combination of the features observed with bias and correlation coefficient.

TABLE I. – *Bias, correlation coefficient and* FSE *of rainfall radar estimates over basins* A *and* B *for* 30 min *rainfall accumulations.*

	Basin A			Basin B		
	bias	ϱ	FSE	bias	ϱ	FSE
R_{ZH}	0.01	0.742	0.709	0.506	0.597	1.083
R_{DR}	− 0.096	0.810	0.683	0.386	0.626	0.982

Table II shows the bias, between radar and gage estimates of rainfall at the several gage locations in basin B for algorithms R_{ZH} and R_{DR}, respectively. We can see from the results of the bias for each gage location that the radar estimate is mostly smaller than the gage measurement (except the last two gages) indicative of potential loss of signal due to beam blockage. For the last two gages the bias is small because at those two gage locations there is no significant beam blockage. R_{DR} algorithm also has significant bias due to beam blockage but the amount of bias is slightly less than R_{ZH}. According to eqs. (8) and (9), it can be seen that a power reduction due to the beam blockage introduces an error on R_{DR} estimates larger than on R_{ZH} estimates. To this purpose, the contradictory results shown in table II can be explained assuming that Z_{DR} values are affected by the beam blockage and/or a residual error due to attenuation correction technique is still present.

One way to correct for the effect of the beam blockage is to estimate the amount of the beam blocked by the mountain ridge. However, this is only an approximate procedure. Nevertheless, if we have large amount of data from one gage location, then we can calibrate the radar beam for beam blockage. To apply this procedure we need long-time record of precipitation observed by a specific gage, so that fairly accurate estimates of bias due to beam blockage can be made. In the basin B gage number 6 (ID 6) received fairly long-time record of precipitation. We evaluate this procedure using data at gage number 6 where we use half the data to estimate the bias and scale the reflectivity value accordingly. This scaling factor is applied to the rest of the data for testing. Without the correction the comparison at gage number 6 had a bias of 0.73 (indicating excessive beam blockage) and correlation coefficient 0.86. The FSE of the rainfall comparison for 15 min average was 0.92. When the correction is done, the new

TABLE II. – *Bias between radar and gage estimates of rainfall for the various gages over basin* B.

Bias		
Gages (ID)	R_{ZH}	R_{DR}
5	0.615	0.529
6	0.658	0.459
7	0.436	0.307
8	0.496	0.494
9	0.054	− 0.005
15	0.134	0.05

radar estimates have FSE of 0.5, bias 0.38 and correlation coefficient of 0.93. We can see from the result for gage number 6, the bias is significantly reduced (more than 50%). Thus this procedure can be applied to correct the radar estimates of rainfall using gage measurements at locations of beam blockage. We emphasize that we still use one Z-R equation for the entire basin.

6. – Summary and conclusion

Intercomparison radar and gage maeasurements of rainfall over the Central Apennines is presented in this paper. Radar operations for precipitation estimation in mountainous regions is constrained by the requirements of avoiding beam blockage as well as contamination by the melting layer. The raingage measurements and radar estimates of rainfall over two distinct locations in the Apennines are compared to study the effect of beam blockage on radar measurements. The radar estimates of rainfall are obtained using two different algorithms, namely *a*) using reflectivity only, and *b*) using dual-polarization algorithm. The fractional standard error (%), bias and correlation coefficient of the comparison between the raingage measurements and the radar estimates with the two algorithms are studied over the two basins A and B. The radar scans over basin B are significantly affected by beam blockage in comparison to basin A. For both basins A and B the FSE of R_{DR} was less than that of R_{ZH}. It is to be noted here that the same rainfall algorithm is used for both regions A and B. The fractional standard error and the bias between gage and radar estimates of rainfall are higher for basin B in comparison to basin A. In addition, the correlation coefficient between the radar and gage measurements of rainfall are higher for basin A in comparison to basin B.

A simple procedure is developed to estimate the bias in the radar rainfall estimates due to beam blockage from part of the data. This bias is utilized to estimate the percentage of beam blockage by the mountain ridges and, correspondingly, correct the radar estimates of rainfall. This simple correction procedure significantly reduced the bias as well as the fractional standard error in the rainfall estimates. In addition, the correlation coefficient between the radar and gage estimates also improved. Thus it appears that it is potentially possible to estimate rainfall over mountainous regions in the presence of beam blockage using same radar rainfall algorithms that are derived in ideal conditions.

* * *

This research was supported partially by the National Group for Defence from Hydrogeological Hazards (CNR, Italy), by Italian Space Agency (ASI), by Mesoscale Alpine Project (MAP-CNR) and by NASA (TRMM). The authors are grateful to Mr. P. IACOVELLI for drafting and typing.

REFERENCES

[1] SELIGA T. A. and BRINGI V. N., *Potential use of the radar reflectivity at orthogonal polarizations for measuring precipitation, J. Appl. Meteorol.*, **15** (1976) 69-76.

[2] SCARCHILLI G., GORGUCCI E., CHANDRASEKAR V. and SELIGA T. A., *Rainfall estimation using polarimetric techniques at C-band frequencies, J. Appl. Meteorol.*, **32** (1993) 1150-1159.

[3] GORGUCCI E., SCARCHILLI G. and CHANDRASEKAR V., *A robust estimator of rainfall rate using differential reflectivity, J. Atmos. Ocean. Technol.*, **11** (1994) 586-592.
[4] ULBRICH C. W., *Natural variations in the analytical form of raindrop size distributions, J. Climate Appl. Meteorol.*, **22** (1983) 1764-1775.
[5] BRINGI V. N., CHANDRASEKAR V., BALAKRISHNAN N. and ZRNIC D. S., *An examination of propagation effects in rainfall on radar measurements at microwave frequencies, J. Atmos. Ocean. Technol.*, **7** (1990) 829-840.
[6] AYDIN K., ZHAO Y. and SELIGA T. A., *Rain-induced attenuation effects on C-band dual-polarization meteorological radars, IEEE Trans. Geosci. Remote Sens.*, **27** (1989) 57-66.
[7] SCARCHILLI G., GORGUCCI E., GIULI D., FACHERIS L., FRENI A. and VEZZANI G., *Arno project: Radar system and objectives*, in *XXV Conference on Radar Meteorology, Paris, France, 1991* (American Meteorology Society), pp. 805-808.
[8] AYDIN K., SELIGA T. A. and BALAJI V., *Remote sensing of hail with a dual-linear polarization radar, J. Climate Appl. Meteorol.*, **25** (1986) 1475-1484.